Biosensors and Bioelectronics 32 (2012) 37–42

Contents lists available at SciVerse ScienceDirect

Biosensors and Bioelectronics

journal homepage: www.elsevier.com/locate/bios

Ultrasensitive electrogenerated chemiluminescence biosensor for the determination of mercury ion incorporating G4 PAMAM dendrimer and Hg(II)-specific oligonucleotide

Fen Ma[a], Yu Zhang[a], Honglan Qi[a], Qiang Gao[a], Chengxiao Zhang[a,*], Wujian Miao[b,**]

[a] Key Laboratory of Applied Surface and Colloid Chemistry, Ministry of Education, School of Chemistry and Materials Science, Shaanxi Normal University, Xi'an, 710062, PR China
[b] Department of Chemistry and Biochemistry, The University of Southern Mississippi, Hattiesburg, MS 39406, USA

ARTICLE INFO

Article history:
Received 9 August 2011
Received in revised form 6 November 2011
Accepted 7 November 2011
Available online 7 December 2011

Keywords:
Electrogenerated chemiluminescence
Biosensor
Mercury-specific oligonucleotide
Mercury ion
Dendrimer

ABSTRACT

A novel electrogenerated chemiluminescence (ECL) biosensor for highly sensitive and selective detection of mercury ion was developed on the basis of mercury-specific oligonucleotide (MSO) served as a molecular recognition element and the ruthenium(II) complex (Ru1) as an ECL emitting species. The biosensor was fabricated on a glassy carbon electrode coated with a thin layer of single wall carbon nanotubes, where the ECL probe, NH_2-$(CH_2)_6$-oligo(ethylene oxide)$_6$-MSO ↔ Dend-Ru1, was covalently attached. The Dend-Ru1 pendant was prepared by covalent coupling Ru1 with the 4th generation polyamidoamine dendrimer (Dend), in which each dendrimer contained 35 Ru1 units so that a large amplification of ECL signal was obtained. Upon binding of Hg^{2+} to thymine (T) bases of the MSO, the T–Hg–T structure was formed, and the MSO changed from its linear shape to a "hairpin" configuration. Consequently, the Dend-Ru1 approached the electrode surface resulting in the increase of anodic ECL signal in the presence of the ECL coreactant tri-*n*-propylamine. The reported biosensor showed a high reproducibility and possessed long-term storage stability (92.3% initial ECL recovery over 30 day's storage). An extremely low detection limit of 2.4 pM and a large dynamic range of 7.0 pM to 50 nM Hg^{2+} were obtained. An apparent binding constant of $1.6 \times 10^9\ M^{-1}$ between Hg^{2+} and the MSO was estimated using an ECL based extended Langmuir isotherm approach involving multilayer adsorption. Determination of Hg^{2+} contents in real water samples was conducted and the data were consistent with the results from cold vapor atomic fluorescence spectroscopy.

1. Introduction

Electrogenerated chemiluminescence (ECL) biosensors combine the advantages of both electrochemical and chemiluminescent biosensors, and are highly sensitive, easy to control and operate with inexpensive equipment, and exceedingly selective due to the use of the biological recognition element in conjunction with specific ECL label and coreactant. In order to further improve the sensitivity of the ECL biosensor, great efforts have been made employing nanomaterials as a carrier in recent years. For example, by using micro-sized polystyrene beads (PSBs) (Miao and Bard, 2004), or silica nanoparticles (Si-NPs) (Wei et al., 2008) as the carrier of a large amount of ECL labels, remarkable amplification in ECL intensity for each bio-event (e.g., DNA hybridization, antibody-antigen interaction) was observed. However, the use of non-aqueous media for PSBs-based ECL measurement and the non-conductivity of the Si-NPs limit their further effective applications and development in biorelated areas.

Dendrimers are a family of nano-sized, three-dimensional polymers characterized by a unique tree-like branching architecture and compact spherical geometry in solution (Medina and El-Sayed, 2009). They have been used for many diverse applications within the biological, chemical, polymer, and nanotechnology fields. For example, dendrimers have been used as carriers of affinity ligands, and as additives for other polymer mixtures due to their intrinsic and exciting properties, such as, water-solubility, highly geometric symmetry, chemical stability, and surface functionality (Takada and Abruña, 2004). The preparation and properties of $Ru(bpy)_3^{2+}$ pendant poly(amidoamine) (PAMAM) dendrimers and $Ru(tpy)_2^{2+}$ (tpy = terpyridyl) pendant PAMAM dendrimers were reported (Storrier et al., 1999). The ECL intensity of carbosilane dendrimer covalently linked with eight $Ru(bpy)_3^{2+}$ units in tri-*n*-propylamine (TPrA)-MeCN solution was reported to be five folds higher than that of the $Ru(bpy)_3^{2+}$ standard (Zhou and

* Corresponding author. Tel.: +86 29 8530 3825; fax: +86 29 8530 7774.
** Corresponding author. Tel.: +1 601 266 4716; fax: +1 601 266 6075.
E-mail addresses: cxzhang@snnu.edu.cn (C. Zhang), wujian.miao@usm.edu (W. Miao).

0956-5663/$ – see front matter © 2011 Elsevier B.V. All rights reserved.
doi:10.1016/j.bios.2011.11.011

Roovers, 2001). Recently, an ECL assay for cancer cells based on dendrimer/CdSe-ZnS-quantum dot nanoclusters was reported (Jie et al., 2011). However, to our best knowledge, PAMAM dendrimers have not been employed as the carrier of $Ru(bpy)_3^{2+}$/TPrA system combined with DNA in the field of ECL biosensors.Hg^{2+} is one of the highly toxic environmental pollutants (Risher, 2003) and microbial biomethylation of Hg^{2+} yields methyl mercury that could be accumulated in the body through the food chain and cause health problems such as brain damage and other chronic diseases (Nolan and Lippard, 2008). Determination of Hg^{2+} can be achieved with a numbers of traditional analytical approaches, which include atomic absorption or emission spectroscopy (Butler et al., 2010), inductively coupled plasma-mass spectrometry (Leermakers et al., 2005) and selective cold vapor atomic fluorescence spectrometry (Bloom and Fitzgerald, 1988). These methods are sensitive but generally involve tedious sample preparation, expensive and sophisticated instrumentation which significantly limit their portability. As a result, several alternative designs based on the highly specific interaction of Hg^{2+} with thymine (T) (Miyake et al., 2006) for sensitive Hg^{2+} detection using, e.g., optical (Dave et al., 2010; Ono and Togashi, 2004), electrochemical (Zhu et al., 2009; Liu et al., 2009), and ECL biosensors was recently reported (Zhu et al., 2010; Tang et al., 2010). Although the above ECL biosensors showed a very low Hg^{2+} detection limit of 2.3 nM and 20 pM, respectively, the fabricated biosensors cannot be reused, as the Au—S bond formed between the Au electrode and the thiolated DNA was damaged after the initial anodic potential cycling.

In this study, a new type of Hg^{2+} selective ECL biosensor with extremely low detection limit and high stability and long-term storage is presented. Scheme 1 illustrates the working principle of the biosensor. The Hg^{2+} specific oligonucleotide (MSO) is covalently attached to the surface of carboxylated single-wall carbon nanotubes (SWNTs) on a glassy carbon electrode via an appropriate length of spacer. G4 PAMAM dendrimer with heavily loaded $Ru(bpy)_3^{2+}$ derivatives is tethered to the other end of the MSO. In the presence of Hg^{2+}, the initial linear MSO bends to form a "hairpin" type structure after the complexation reaction between Hg^{2+} and thymine bases, which leads to the ECL labels become closer to the electrode surface. As a result, a significant increase in ECL intensity is expected with the Hg^{2+} bound ECL biosensor upon the anodic potential scanning or pulsing in the presence of TPrA. A number of factors that could affect the performance of the Hg^{2+} ECL biosensor, including the signal amplification effect of SWNTs and Dend-Ru1, the length of the spacer, and the surface coverage of the MSO, will be investigated. The fabricated ECL biosensor is validated by applying it to measuring the Hg^{2+} contents in real water samples.

2. Experimental

2.1. Reagents

Bis(2,2′-bipyridine)-4′-methyl-4-carboxybipyridine-ruthenium (*N*-succinimidyl ester)-bis (hexafluorophosphate) (abbreviated Ru1, see Supplementary data, Scheme S1), ethylenediamine core poly (amidoamine) dendrimers (PAMAM dendrimers, generation 4 with 64 surface primary amino groups, 10 wt.% in methanol), *N*-(3-dimsethylaminopropyl)-*N*-ethylcarbodiimide hydrochloride (EDC), and *N*-hydrosuccinimide (NHS, 98%) were purchased from Sigma-Aldrich (USA). Bis(2,2′-bipyridine)-4′-methyl-4-carboxybipyridine-ruthenium-ethylenediamine-bis (hexafluophosphate) (abbreviated as Ru2, see Supplementary data, Scheme S2) was synthesized on the basis of our previous report (Li et al., 2007). Carboxyl single-wall carbon nanotubes (SWNTs, ~30 μm long, —COOH content 2.73 wt.%) were obtained from Shenzhen Nanotech Port Co., Ltd. (China). Humic acid was purchased from Shanghai Lanyuan Bio Inc. (China). 4-(2-hydroxyerhyl)piperazine-1-erhanesulfonic acid (HEPES) from Bio Basic (Canada), tri-*n*-propylamine (TPrA) from Sinopharm Chemical Reagent Co., Ltd. (China), *N*,*N*-dimethylformamide (DMF) from Xi'an Chemical Reagent Factory (China), dimethyl sulfoxide (DMSO) from Tianli Chemical Reagent Co., Ltd. (China), and mercuric nitrate ($Hg(NO_3)_2{\cdot}1/2H_2O$) from Taixing Reagent Factory (China), respectively, were all of analytical grade and used as received.

A 22-mer mercury (II)-specific oligonucleotide, 5′-TTC TTT CTT CCC CTT GTT TGT T-3′, was used as reported previously (Ono and Togashi, 2004). Other sequences used were obtained via custom synthesis from Shanghai Sangon Biological Engineering Technology & Services Co., Ltd. (China), which included 5′-HPO_4^--MSO-$(CH_2)_6$-NH_2-3′, 5′-NH_2-$(CH_2)_6$-MSO-HPO_4^--3′, and 5′-NH_2-$(CH_2)_6$-$OP(O)_2O$-$(CH_2CH_2O)_n$-$P(O)_2O$-MSO-HPO_4^--3′ ($n = 0, 3, 6, 9$).

2.2. Synthesis of Dend-Ru1 and NH_2-C_6-$(EG)_6$-MSO ↔ Dend-Ru1

The PAMAM dendrimers carried with Ru1 (Dend-Ru1) was synthesized according to the procedure from the literature (Schlapak et al., 2007) with a modification. Briefly, 1.5 mg (0.11 μmol) of PAMAM dendrimers was added to 100 μL of DMSO containing 4.9 μmol of Ru1, stirring for 12 h at ~25 °C, and then the mixture solution was diluted with 1 mL of water. The remaining unreacted Ru1 was separated from the dendrimer coupled Ru1 product via a dialysis process against water at 4 °C using cellulose dialysis membrane (cutoff M.W.: 1.4 kDa, Bio Basic Inc., Canada). The obtained Dend-Ru1 solution was then lyophilized for further use.

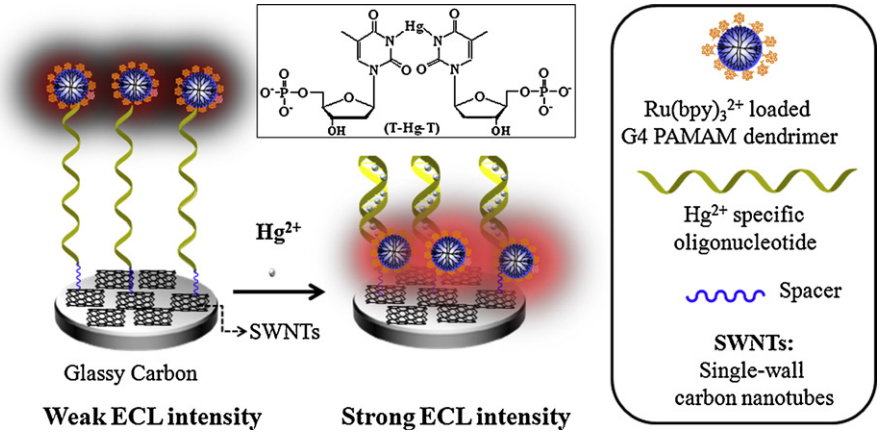

Scheme 1. Working principle of the Hg^{2+} ECL biosensor.

The ECL probe (NH_2-C_6-$(EG)_6$-MSO ↔ Dend-Ru1) was synthesized with the procedure reported in our previous work (Ma et al., 2011) with a modification. Briefly, 500 μL of freshly prepared 10 mM EDC, 500 μL of 0.10 M imidazole (pH 6.0), and 13 μL of 1.06 mM Dend-Ru1 (13.8 nmol) were mixed with 400 μL of DNA buffer containing 5 OD (OD = "optical density"; 1 OD at 260 nm ≈33 μg/mL ssDNA) of NH_2-C_6-$(EG)_6$-MSO (13 nmol). The reaction was performed for ~12 h at room temperature under gentle shaking. Subsequently, 12 mg of succinic anhydride was added to the reaction mixture so that ~50% of the surface amine groups of Dend-Ru1 were blocked and converted into negatively charged carboxylates during a 24 h reaction period (Hermanson, 1996). Finally, the mixture was passed through a Sephadex G-25 column to collect the ECL probe from the solution matrix. With similar procedures, NH_2-C_6-$(EG)_n$-MSO ↔ Dend-Ru1 conjugates (n = 0, 3, 9) were also synthesized.

2.3. Fabrication of ECL biosensors

2.0 mg of SWNTs was ultrasonically dispersed in 2.0 mL of DMF, and 10 μL of which was drop-coated onto the surface of a glassy carbon electrode (GCE, 2 mm diameter). The air-dried GCE was immersed into 1.0 mL of freshly prepared 5 mM EDC and 8 mM NHS for 30 min and then rinsed with 50 mM HEPES buffer (pH 7.4). Subsequently, the electrode with activated carboxyl SWNTs was immersed into 400 μL of 2.0 μM ECL probe for 1 h at 28 °C and then deactivated by dropping a 30 μL of 1.0 mM ethanolamine for 15 min. The obtained electrode used as the ECL biosensor was finally rinsed thoroughly with DNA buffer and stored in air at 4 °C in the dark before use.

2.4. ECL measurement

The ECL biosensor fabricated was immersed in 200 μL of a Hg^{2+} solution for 30 min at ~35 °C, followed by extensively rinsing with 50 mM HEPES buffer (pH 7.4) to remove any physically adsorbed Hg^{2+}. And then, the Hg^{2+}-bound biosensor was placed in an ECL cell containing 3.0 mL of 0.10 M TPrA-50 mM HEPES (pH 7.4). The ECL measurement was performed at a constant potential of +1.30 V vs Ag/AgCl. The concentration of Hg^{2+} was quantified on the basis of the ECL peak intensity change, $\Delta I = I - I_0$, where I_0 and I were the ECL peak intensity before and after the ECL biosensor was interacted with Hg^{2+}, respectively.

3. Results and discussion

3.1. ECL behavior of Ru1 and Dend-Ru1

Fig. 1 shows ECL-potential curves of Ru1 and Dend-Ru1 at a GCE. Both ECL profiles display the characteristic ECL behavior of the aqueous $Ru(bpy)_3^{2+}$/TPrA system (Miao et al., 2002). The ECL intensity obtained from Ru1 solution at ~1.17 V is ~1.7 times stronger than that of Dend-Ru1 at ~1.20 V although the two tested solutions have the same Ru1 concentration of 10 μM since each Dend-Ru1 contains 35 Ru1 units (see Supplementary data, Fig. S1 and elemental analysis). In other words, the ECL efficiency of each dendrimer bound Ru1 is ~59% of that obtained from the free Ru1. This may be ascribed to the following three factors. First, the large Dend-Ru1 cluster results in its slow diffusion to the electrode and its retarded reaction of the bulky oxidized Dend-Ru1 with the TPrA radicals (Zhou and Roovers, 2001). Second, the salvation property of the Ru1 in dendrimer could be different from that of the free Ru1 in solution. With the increase of dendrimer generation, the solvent around the pendant $Ru(bpy)_3^{2+}$ groups has been found to be increasingly filled by the branches of the dendrimer with the simultaneous displacement of the bulk solvent molecules (Glazier et al., 2003).Third, self-quenching of the Ru1 ECL emitter within Dend-Ru1 complex could also occur as the distance between adjacent Ru1 species is small (Barron et al., 2003). Not surprisingly, the ECL from Dend-Ru1 is generated at a slightly positive potential region (~30–100 mV) as compared with that from free Ru1. Fig. 1 also demonstrates that when a Dend-Ru1 cluster with 35 Ru1 units is used as a single label in ECL-related analysis, ~21-fold increase in ECL intensity with respect to a Ru1 label can be obtained. This provides a promising strategy for amplifying the ECL intensity in our present study in aqueous media. As a result, the sensitivity of the ECL biosensor established on the basis of Dend-Ru1 and the limit of detection of the target analyte are expected to be improved significantly.

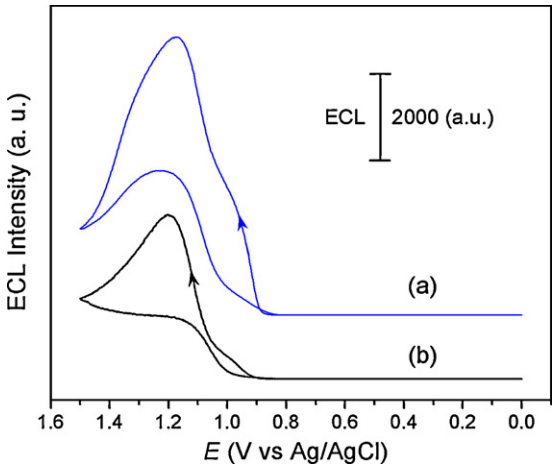

Fig. 1. ECL-potential curves of Ru1 and Dend-Ru1. (a) 10 μM Ru1; (b) 0.29 μM Dend-Ru1 in 50 mM HEPES buffer (pH 7.4) containing 50 mM TPrA at a GC electrode at a scan rate of 20 mV/s.

3.2. Design and characterization of the ECL biosensor

To investigate the signal amplification effect of SWNTs and Dend-Ru1 on the ECL biosensor, the ECL biosensor (GCE/SWNTs/NH_2-C_6-$(EG)_6$-MSO ↔ Dend-Ru1) and four other types of ECL biosensors, namely, Type A (GCE/SWNTs/G4 PAMAM/MSO-C_6-NH_2 ↔ Ru1), Type B (GCE/SWNTs/NH_2-C_6-MSO ↔ Ru2), Type C (GCE/NH_2-C_6-$(EG)_6$-MSO ↔ Dend-Ru1) and Type D (GCE/NH_2-C_6-MSO ↔ Ru2), were fabricated and examined. Among the five biosensors, the ECL biosensor gives the highest ECL intensity change (ΔI = 10,096 (a.u.)), whereas the signals from Type C (ΔI = 62) and Type D (ΔI = 50) are very weak. This is attributed to the fact that without using SWNTs, $Ru(bpy)_3^{2+}$ containing labels are attached to GCE via physical adsorption only, while the three other biosensors involve covalent bonding between SWNTs and remaining ECL labels. Additionally, SWNTs can increase the active surface area of the GCE. For SWNTs based biosensors, when the multiple $Ru(bpy)_3^{2+}$-loaded dendrimer, Dend-Ru1, is used as an ECL label, ΔI_{ECL} is increased by ~10 times with respect to that obtained from biosensors using Ru1 as ECL label for Type A (ΔI = 1139) and Ru2 for Type B (ΔI = 723). As a result, the ECL biosensor that consists of GCE/SWNTs covalently bound to MSO linked Dend-Ru1 was chosen to be the ECL probe.

In order to reduce the blank signal of the ECL biosensor and facilitate the access of Hg^{2+} to the ECL biosensor probe binding sites, alkyl carbon chain —$(CH_2)_6$ and oligo(ethylene oxide) (abbreviated, EG) were used as a spacer to adjust the distance of the MSO to the surface of the GCE/SWNTs, so that the ΔI_{ECL} value can be maximized. For the biosensors with a common configuration of GCE/SWNTs/NH_2-C_6-$(EG)_n$-MSO ↔ Dend-Ru1), the length of

the ECL probe (i.e., NH_2-C_6-$(EG)_n$-MSO) was estimated to be 82.5, 103.5, 111.7, and 136.0 Å when n = 0, 3, 6, and 9, respectively, where ~74.8 Å was attributed to the MSO sequence (~3.4 Å/base) (Lao et al., 2009). The result showed that the blank ECL intensity (I_0, in a.u.) of 6325, 3928, 1120 and 879, and the sample ECL intensity (I, in a.u.) of 8456, 9326, 11210 and 8213 after the biosensors were treated with Hg^{2+}, were obtained with n = 0, 3, 6, and 9, respectively. As for the ECL intensity change (ΔI_{ECL}), with n increases from 0, 3, 6, to 9, the relative ΔI_{ECL} value varies from 21.1%, 53.5%, 100%, to 72.7%, respectively. The decrease of I_0 with increase of the ECL probe length is because the longer the probe is, the larger the spacer resistance will be, and the harder the $Ru(bpy)_3^{2+}$ and TPrA get oxidized (Pittman and Miao, 2008). The biosensor with n = 6 demonstrated the maximum I and ΔI_{ECL}. Two opposing processes could have occurred. On the one hand, an increase in probe length could move the MSO away from the electrode surface into a more solvated environment, which results in reduced steric hindrance for Hg^{2+} to approach and bind to the MSO, causing an increased binding efficiency. The Dend-Ru1 tag could thus be closer to the electrode surface after the efficient formation of Hg^{2+} induced hairpin structural conformation of the MSO, which is favorable to the ECL generation. It could be also possible that more negative charges in the spacer (EG) could reduce the rate of duplex formation, which could affect the interaction between MSO and Hg^{2+} and further decrease the ECL intensity. NH_2-C_6-$(EG)_6$-MSO ↔ Dend-Ru1, therefore, was chosen as the ECL biosensor probe.

The surface coverage of the ECL probe on GCE/SWNTs, is expected to affect the ECL intensity of the biosensor towards Hg^{2+} detection, because a low surface coverage corresponds to a limited number of Ru1 available for ECL generation, whereas a highly condensed surface coverage could sterically hinder the formation of the MSO–Hg^{2+} hairpin structure, especially given the fact that Dend-Ru1 is a very large unit with a diameter of ~66.2 Å which can be estimated on the basis of the diameter of G4 PAMAM dendrimer (about 45 Å) (Esumi et al., 2003) and Ru1 (estimated 10.6 Å by ChemBio 3D Ultra). Since the ECL probe concentration directly influence the surface coverage of the ECL probe on GCE/SWNTs, the probe concentration for fabrication of the biosensor is optimized. Fig. 2 shows the dependence of the ECL intensity of the biosensor on the concentration of the ECL probe. The nearly steady state ECL intensity is observed from the bare and the Hg^{2+} bound biosensor when a probe concentration of 5.0 μM or above is used, which suggests that the GCE/SWNTs surface is saturated with the probes. The maximum ECL intensity occurs at the probe concentration of

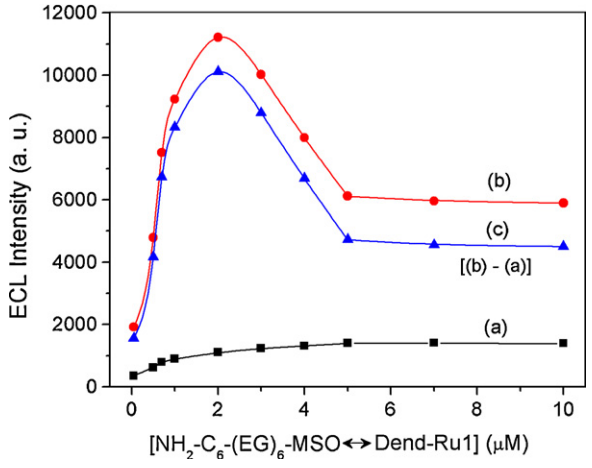

Fig. 2. Dependence of the ECL intensity of the biosensor on the concentration of the ECL probe employed during the biosensor fabrication at a given reaction time of 1 h at 28 °C. (a) before and (b) after treated with 1.0 nM Hg^{2+}, (c) ECL intensity change. The ECL was carried out in 0.10 M TPrA-50 mM HEPES buffer (pH 7.4) at 1.30 V.

2.0 μM, which is consistent with our earlier prediction. That is, the obtained surface coverage of the ECL probe on GCE/SWNTs is high enough but not crowded under present experimental conditions. The ECL biosensor was also characterized by cyclic voltammetry, confirming that the ECL biosensor was successfully fabricated and can be used to determine Hg^{2+} (Fig. S2).

3.3. Optimization of test conditions

To maximize the ECL performance of the biosensor for Hg^{2+} detection, the applied potential and the incubation time of the biosensor with Hg^{2+} analyte were examined. The ECL intensity of the Hg^{2+} bound biosensor is a function of the potential, in which a peak ECL is located at the applied potential of 1.30 V (Fig. S3). In order to generate sufficient ECL, both solution-phase TPrA and surface-confined Dend-Ru1 must be effectively oxidized. The solution-phase Dend-Ru1 has shown a maximum ECL at ~1.20 V. A slightly more positive potential is expected for the oxidation of the tethered Dend-Ru1 within the biosensor, as NH_2-C_6-$(EG)_6$-MSO linker requires additional potential to compensate the *IR* drop. With the further increase of the applied potential, however, ΔI_{ECL} decreases. This could be related to the oxidation of water that produces extra amounts of oxygen, resulting in the consumption of $TPrA^{\bullet}$ free radicals needed for the generation of the excited state $Ru1^*$ species (Miao and Bard, 2004).

The dependence of the ECL intensity on the interaction time between the biosensor and Hg^{2+} (1.0 nM) was investigated. A nearly linear increase in ECL intensity is observed with an incubation time of 5–25 min, which is followed by a stabilized ECL signal at a longer time of 30–60 min (Fig. S4). The critical incubation time of 30 min, which was chosen in the present study for Hg^{2+} detection, is slightly longer than that required for homogenous fluorescent (10 min) (Wang et al., 2008) and colorimetric (20 min) Hg^{2+} detection (Li et al., 2008). However, this incubation time is much shorter than that needed for electrochemical based Hg^{2+} selective biosensors (~1 h) (Zhu et al., 2009; Liu et al., 2009), which is probably due to the fact that the use of $(EG)_6$ spacer in the current study has significantly improved the binding efficiency between Hg^{2+} and the MSO as discussed earlier.

The appropriate ionic strength is important for the configuration of the ECL probe and the stability of its complexation with Hg^{2+}. The dependence of the ECL intensity on the ionic strength was investigated. The ECL intensity increased with the increase of $NaNO_3$ concentration from 0.020 M to 0.10 M (see Supplementary data, Fig. S5). This is probably due to the fact that the MSO is a negatively charged biopolymer, its folding strongly depends on the presence of cations such as Na^+ to neutralize the negatively charged backbone. With the further increase of the concentration of $NaNO_3$ from 0.10 M to 1.0 M, however, the ECL intensity decreased. In this case, the decreased in Hg^{2+} activity due to the increase in ionic strength may have played a dominated role. As a result, 0.10 M $NaNO_3$ was chosen in the present work to maximize the ECL intensity.

3.4. Performance of the biosensor

Fig. 3A shows the ECL profiles obtained from the biosensor with different concentrations of Hg^{2+} in the presence of 0.10 M TPrA. As shown in Fig. 3B, the ECL peak intensity is [Hg^{2+}] dependent, in which a well-fitted linear correlation between the ECL peak intensity change and the logarithm of the Hg^{2+} concentration across over four orders of concentration range (7.0×10^{-12} to 5.0×10^{-8} M) is evident. Such a wide dynamic range is ~2–3 orders of magnitude larger than that from other previously reported methods based on T–Hg^{2+}–T interactions, which include electrochemical biosensors (Zhu et al., 2009; Liu et al., 2009), colorimetry with gold nanoparticles (Lee et al., 2007), and fluorescent probes based

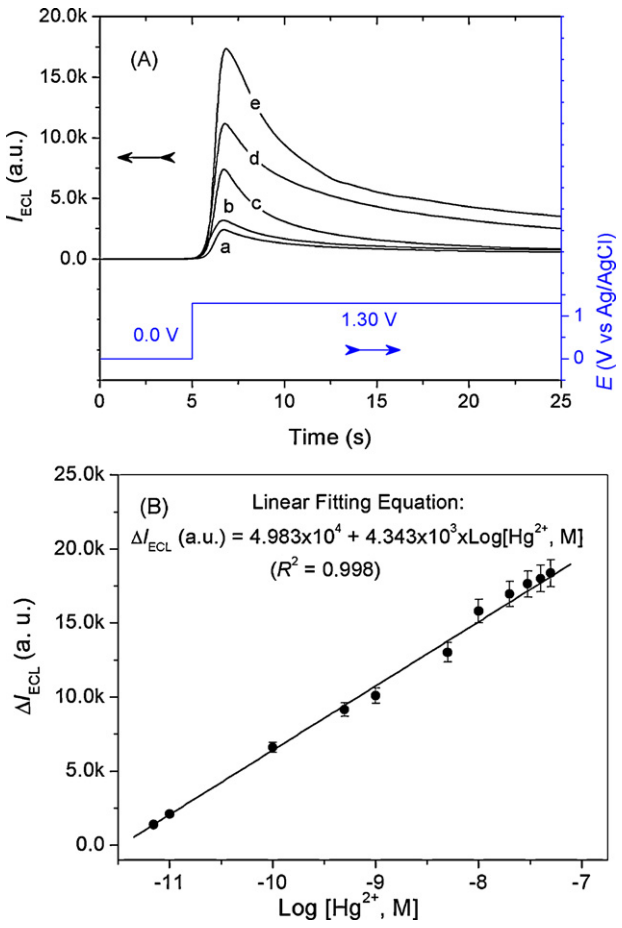

Fig. 3. (A) ECL responses of the biosensor after treated with different concentrations of Hg^{2+}. (a) 7.0, (b) 10.0, (c) 100.0, (d) 1000.0 and (e) 10,000.0 pM. (B) Linear relationship between the ECL peak intensity change and the Hg^{2+} concentration. Conditions for ECL measurements were the same as in Fig. 2.

on a DNAzyme catalytic beacon (Liu and Lu, 2007). The obtained detection limit of 2.4 pM (defined as S/N = 3) is about 8 and 97 times lower than that from the ECL biosensors on the basis of the interaction of $Ru(phen)_3^{2+}$ into dsDNA (Tang et al., 2010) and the oligonucleotides labeled $Ru(bpy)_3^{2+}$-doped silica nanoparticles (Zhu et al., 2010), respectively. This detection limit is much lower than the allowed maximum contaminant level of inorganic mercury in drinking water (2 ng/L or 10 nM) legally enforced by the US EPA (Office of Water, 2009). The reproducibility of the biosensors fabricated using the GCEs (2 mm diameter) with same surface area was examined. The relative standard deviations were 5.2% for one GCE and 4.0% for a batch GCEs (0.1 nM Hg^{2+}, $n = 7$), respectively. The ultra-sensitivity and reproducibility of the ECL biosensors for the determination of Hg^{2+} are, therefore, obtained.

The fabricated biosensor also has an excellent selectivity towards Hg^{2+} ions. The ECL responses from 2.0 μM of nine common co-existing divalent metal ions (Cu^{2+}, Zn^{2+}, Cd^{2+}, Pb^{2+}, Fe^{2+}, Co^{2+}, Ni^{2+}, Ca^{2+}, and Ba^{2+}) are in the similar range of the blank, and their ECL intensities are less than 9% of that from 10.0 nM Hg^{2+} (Fig. S6). The effect of Cl^-, SO_4^{2-}, and CO_3^{2-} anions on the ECL response of Hg^{2+} was also investigated. As shown in Fig. S7 in the Supplementary data, these anions at 10 mM respective ion concentration levels have essentially no effect on the ECL response of 1.0 nM Hg^{2+}. The effect of methyl mercury ion (CH_3Hg^+) on the ECL response of Hg^{2+} was examined. The ECL responses from the mixture solutions of 1.0 nM Hg^{2+} and different concentrations of CH_3Hg^+ (up to 1000 nM, Fig. S8 in Supplementary data) show less than −6% in ECL intensity from 1.0 nM Hg^{2+}. These data clearly indicate that co-existing divalent metal ions, Cl^-, SO_4^{2-}, and CO_3^{2-} and CH_3Hg^+ have negligible effect on the ECL response of Hg^{2+}. This is consistent with the fact that the DNA sequence used was a thymine (T)-rich, Hg^{2+} specific oligonucleotide with the formation of a hairpin structure via the Hg^{2+}-mediated coordination of T–Hg^{2+}–T base pairs (Ono and Togashi, 2004). Additionally, the effect of dissolved organic matter (DOM, humic acid was used as a model compound in this work) on the ECL response of Hg^{2+} was also tested. Considering the US EPA standard at 2 ng/mL Hg(II) for drinking water (United States Environmental Protection Agency, 2009), 1 ng/mL (=5 nM) Hg(II) was chosen for interference experiment of humic acid. The tolerable limit of a humic acid was taken as a relative error not greater than 5%. The result showed that less than 500-folds excess of humic acid (500.0 μg/L) did not interfere (Fig. S9 in Supplementary data). The higher concentration of humic acid reduced the ECL response of Hg^{2+}. This is attributed to the fact that humic acid has a strong binding ability for Hg(II) (Gaffney et al., 1996). This also suggests that the application of the ECL biosensor in this work is limited to "dirty" water samples (Ando and Koide, 2011). The tolerable limit of humic acid for the ECL biosensor is maybe enhanced by using oxidative pretreatment of environmental samples with BrCl or N-chlorosuccinimide (Ando and Koide, 2011). To improve the tolerable limit of humic acid for the ECL biosensor is going on in further work.

The regeneration ability of the ECL biosensor was tested using the reference method (Han et al., 2009), in which the biosensor was conveniently regenerated after incubating the used electrode in 10 μM cysteine for 10 min at 45–50 °C, as cystein-Hg^{2+} complex has a much higher affinity constant (~10^{15}–10^{20} M^{-1}) (Hughes, 1957) than the MSO–Hg^{2+} complex (~10^9 M^{-1}, see below). The results showed that less than ±3% change in ECL intensity was observed from an ECL biosensor over six times regeneration (Fig. S10).

The stability of the ECL biosensor was examined after interaction with 1.0 nM Hg^{2+} by multiple cyclic scanning between 0 and +1.5 V vs Ag/AgCl. A relative standard deviation of 2.3% in ECL intensity over 60 potential cycles (Fig. S11) indicates that the present ECL biosensor possesses excellent stability. After being stored in a refrigerator at 4 °C for 21 and 30 days, the biosensor showed a recovery of 96.8% and 92.3% in ECL signal, respectively, where a 1.0 nM Hg^{2+} solution was used for the test. This indicates that the ECL biosensor also has good storage stability.

The application of the ECL biosensor was evaluated via the determination of Hg^{2+} in water samples collected from Qujiangliuyin pond and Qujiangliuyin penstock (Shaanxi Normal University, China). The Hg^{2+} content in the pond estimated by ECL biosensor and cold vapor atomic fluorescence spectrometry (CVAFS) method (see Supplementary data, 1.5) were 9.20 ± 0.03 nM and 8.82 ± 0.03 nM, respectively. The Hg^{2+} content in the penstock estimated by ECL biosensor and CVAFS method were 4.70 ± 0.05 nM and 4.56 ± 0.04 nM, respectively. The relative deviations were 4.3% and 3.1%, respectively, which show that the data obtained with the ECL biosensor are in good agreement with those obtained from the CVAFS method.

3.5. Binding constant of immobilized ECL probe with Hg^{2+}

As shown in Fig. 4a, the experimentally obtained correlation between ΔI_{ECL} and $[Hg^{2+}]$ can be well fitted with an extended Langmuir isotherm (Eq. (1), Zhang and Wang, 2010), in which multilayer adsorption (binding) of Hg^{2+} ions on the biosensor surface is considered:

$$\Delta I_{ECL} = \Delta I_{ECL}^{max} \frac{K_b[Hg^{2+}]}{1 + K_b[Hg^{2+}]} e^{m([Hg^{2+}]/[Hg^{2+}_{max}])} \quad (1)$$

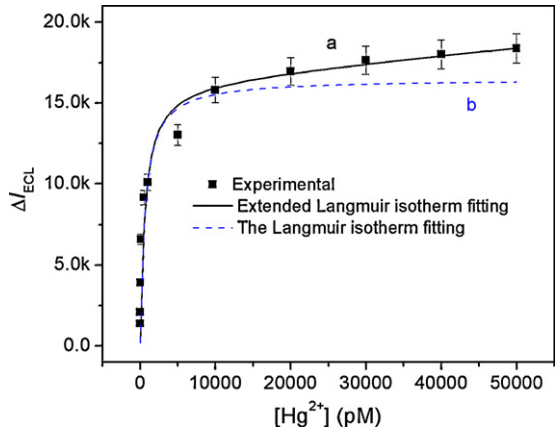

Fig. 4. Langmuir isotherms obtained from the ECL biosensor after interactions with various concentrations of Hg^{2+} at room temperature (~25.0 °C). The experimental data were fitted with (a) an extended Langmuir isotherm, and (b) the simple Langmuir isotherm. The ECL measurement conditions were the same as in Fig. 2.

where ΔI_{ECL}^{max} is the maximum ECL peak intensity change for a monolayer adsorption of Hg^{2+} ions, $[Hg_{max}^{2+}]$ is the maximum concentration of Hg^{2+} present on a monolayer adsorption, and K_b is equivalent to the binding constant between the biosensor and Hg^{2+} for the simple Langmuir isotherm (i.e., $m = 0$ in Eq. (1), Sun et al., 2010; Wang et al., 2009). On the basis of the non-linear fitting of the experimental data with Eq. (1), ΔI_{ECL}^{max}, $[Hg_{max}^{2+}]$, K_b, and m were estimated to be 1.650×10^4 (a.u.), 2.226×10^4 pM, 1.6×10^{-3} pM^{-1} (or 1.6×10^9 M^{-1}), and 0.054, respectively. Since every 22-mer MSO contains seven pairs of T:T bases, each of which could be complexed with one Hg^{2+} ion, it is not surprising that the apparent binding constant obtained from the present study (1.6×10^9 M^{-1}) is much larger than that in solution phase from Hg^{2+} ion specifically bound with one T:T mismatched base pair in duplex DNA (10^6 M^{-1}, Torigoe et al., 2010) as well as with herring sperm DNA ($4.1 \pm 0.3 \times 10^6$ M^{-1}, Li et al., 2006). The result also indicates that the Dend-Ru1 attached to MSO has no obvious effect on the interaction between MSO and Hg^{2+}.

In contrast, a poor fitting curve of the experimental data (Fig. 4b) is obtained with the simple Langmuir equation ($\Delta I_{ECL}^{max} = 1.650 \times 10^4$, $K_b = 1.6 \times 10^{-3}$ pM^{-1}), confirming that each MSO must have multiple sites for Hg^{2+} binding.

The BET isotherm model involving multilayer adsorption (Brunauer et al., 1938, Eq. (2)) was also found to fit the experimental data well (overlapped with Fig. 4a with $\Delta I_{ECL}^{max} = 1.650 \times 10^4$ (a.u.), $K_b = 1.6 \times 10^{-3}$ pM^{-1}, and $[Hg_{max}^{2+}] = 4.324 \times 10^5$ pM, not shown). However, the obtained $[Hg_{max}^{2+}]$ is too large to be experimentally reasonable.

$$\Delta I_{ECL} = \Delta I_{ECL}^{max} \frac{K_b[Hg^{2+}]}{1 + K_b[Hg^{2+}](1 - [Hg^{2+}]/[Hg_{max}^{2+}])}. \quad (2)$$

4. Conclusion

A novel ECL biosensor for highly sensitive determination of Hg^{2+} has been developed on the basis of G4-PAMAM dendrimer as a carrier of the ECL probe. On the basis of an extended Langmuir isotherm equation involving multilayer adsorption, an apparent binding constant of the surface-confined NH_2-C_6-$(EG)_6$-MSO ↔ Dend-Ru1 probe with Hg^{2+} ($K_b = 1.6 \times 10^9$ M^{-1}) was estimated. This ECL biosensor was found to be extremely sensitive, highly selective, and sufficiently accurate towards Hg^{2+} detection and quantification. Examinations on the regeneration ability, the stability over potential cycling, and the storage stability of the biosensor also gave satisfactory results. The strategy presented in this study could be easily extended to various analytical platforms including ECL and electrochemical biosensors as well as lab on chips for the detection of many kinds of analytes or their interactions such as DNA/RNA, DNAzyme/target, aptamer/target, and antibody/antigen.

Acknowledgments

Financial support from the National Natural Science Foundation of China (20975065) and the NSF CAREER award (CHE-0955878) is gratefully acknowledged.

Appendix A. Supplementary data

Supplementary data associated with this article can be found, in the online version, at doi:10.1016/j.bios.2011.11.011.

References

2009 Edition of the Drinking Water Standards and Health Advisories, Office of Water, U.S. Environmental Protection Agency: Washington, DC, 2009.
Ando, S., Koide, K., 2011. J. Am. Chem. Soc. 133, 2556–2566.
Barron, J.A., Bernhard, S., Houston, P.L., Abruña, H.D., Ruglovsky, J.L., Malliaras, G.G., 2003. J. Phys. Chem. A 107, 8130–8133.
Bloom, N., Fitzgerald, W.F., 1988. Anal. Chim. Acta 208, 151–161.
Brunauer, S., Emmett, P.H., Teller, E., 1938. J. Am. Chem. Soc. 60, 309–319.
Butler, O.T., Cairns, W.R.L., Cook, J.M., Davidson, C.M., 2010. J. Anal. At. Spectrom. 25, 103–141.
Dave, N., Chan, M.Y., Huang, P.J.J., Smith, B.D., Liu, J., 2010. J. Am. Chem. Soc. 132, 12668–12673.
Esumi, K., Isono, R., Yoshimura, T., 2003. Langmuir 20, 237–243.
Gaffney, J.S., Marley, N.A., Clark, S.B., 1996. Humic and Fulvic Acids Organic Colloidal Materials in the Environment. American Chemical Society.
Glazier, S., Barron, J.A., Morales, N., Ruschak, A.M., Houston, P.L., Abruña, H.D., 2003. Macromolecules 36, 1272–1278.
Han, B., Yuan, J., Wang, E., 2009. Anal. Chem. 81, 5569–5573.
Hermanson, G.T., 1996. Bioconjugate Techniques. Academic Press, New York.
Hughes, W.L., 1957. Ann. N.Y. Acad. Sci. 65, 454–460.
Jie, G.F., Wang, L., Yuan, J.X., Zhang, S.S., 2011. Anal. Chem. 83, 3873–3880.
Lao, Y.H., Peck, K., Chen, L.C., 2009. Anal. Chem. 81, 1747–1754.
Lee, J.S., Han, M.S., Mirkin, C.A., 2007. Angew. Chem. Int. Ed. 46, 4093–4096.
Leermakers, M., Baeyens, W., Quevauviller, P., Horvat, M., 2005. TrAC Trends Anal. Chem. 24, 383–393.
Li, Y., Jiang, Y., Yan, X.P., 2006. Anal. Chem. 78, 6115–6120.
Li, Y., Qi, H., Fang, F., Zhang, C.X., 2007. Talanta 72, 1704–1709.
Li, D., Wieckowska, A., Willner, I., 2008. Angew. Chem. Int. Ed. 47, 3927–3931.
Liu, J., Lu, Y., 2007. Angew. Chem. Int. Ed. 46, 7587–7590.
Liu, S.J., Nie, H.G., Jiang, J.-H., Shen, G.-L., Yu, R.Q., 2009. Anal. Chem. 81, 5724–5730.
Ma, F., Sun, B., Qi, H., Zhang, H., Gao, Q., Zhang, C.X., 2011. Anal. Chim. Acta 683, 234–241.
Medina, S.H., El-Sayed, M.E.H., 2009. Chem. Rev. 109, 3141–3157.
Miao, W., Bard, A.J., 2004. Anal. Chem. 76, 5379–5386.
Miao, W., Choi, J.P., Bard, A.J., 2002. J. Am. Chem. Soc. 124, 14478–14485.
Miyake, Y., Togashi, H., Tashiro, M., Yamaguchi, H., Oda, S., Kudo, M., Tanaka, Y., Kondo, Y., Sawa, R., Fujimoto, T., Machinami, T., Ono, A., 2006. J. Am. Chem. Soc. 128, 2172–2173.
Nolan, E.M., Lippard, S.J., 2008. Chem. Rev. 108, 3443–3480.
Ono, A., Togashi, H., 2004. Angew. Chem. Int. Ed. 43, 4300–4302.
Pittman, T.L., Miao, W., 2008. J. Phys. Chem. C 112, 16999–17004.
Risher, J.F., 2003. Elemental Mercury and Inorganic Mercury Compounds:. Human Health Aspects; World Health Organization, Geneva.
Schlapak, R., Armitage, D., Saucedo-Zeni, N., Latini, G., Gruber, H.J., Mesquida, P., Samotskaya, Y., Hohage, M., Cacialli, F., Howorka, S., 2007. Langmuir 23, 8916–8924.
Storrier, G.D., Takada, K., Abruña, H.D., 1999. Langmuir 15, 872–884.
Sun, B., Qi, H., Ma, F., Gao, Q., Zhang, C., Miao, W., 2010. Anal. Chem. 82, 5046–5052.
Takada, K., Abruña, H.D., 2004. J. Electroanal. Chem. 567, 249–256.
Tang, C.X., Zhao, Y., He, X.W., Yin, X.B., 2010. Chem. Commun. 46, 9022–9024.
Torigoe, H., Ono, A., Kozasa, T., 2010. Chem. Eur. J. 16, 13218–13225.
United States Environmental Protection Agency, EPA 816-F-09-004, 2009.
Wang, Z., Lee, J.H., Lu, Y., 2008. Chem. Commun. 600, 5–6007.
Wang, S., Milam, J., Ohlin, A.C., Rambaran, V.H., Clark, E., Ward, W., Seymour, L., Casey, W.H., Holder, A.A., Miao, W., 2009. Anal. Chem. 81, 4068–4075.
Wei, H., Liu, J., Zhou, L., Li, J., Jiang, X., Kang, J., Yang, X., Dong, S., Wang, E., 2008. Chem. Eur. J. 14, 3687–3693.
Zhang, P., Wang, L., 2010. Sep. Purif. Technol. 70, 367–371.
Zhou, M., Roovers, J., 2001. Macromolecules 34, 244–252.
Zhu, Z., Su, Y., Li, J., Li, D., Zhang, J., Song, S., Zhao, Y., Li, G., Fan, C., 2009. Anal. Chem. 81, 7660–7666.
Zhu, X., Chen, L., Lin, Z., Qiu, B., Chen, G., 2010. Chem. Commun. 46, 3149–3151.